NeuroImage 48 (2009) 269–279

Contents lists available at ScienceDirect

NeuroImage

journal homepage: www.elsevier.com/locate/ynimg

Repetition suppression and plasticity in the human brain

Marta I. Garrido [a,b,*], James M. Kilner [a], Stefan J. Kiebel [c], Klaas E. Stephan [a,d], Torsten Baldeweg [e], Karl J. Friston [a]

[a] Wellcome Trust Centre for Neuroimaging, Institute of Neurology, University College London, UK
[b] Department of Psychology, University California, Los Angeles, USA
[c] Max Planck Institute for human cognitive and brain sciences, Leipzig, Germany
[d] Laboratory for Social and Neural Systems Research, Institute for Empirical Research in Economics, University of Zurich, Switzerland
[e] Developmental Cognitive Neuroscience, Institute of Child Health, University College London, UK

ARTICLE INFO

Article history:
Received 9 October 2008
Revised 28 April 2009
Accepted 15 June 2009
Available online 21 June 2009

Keywords:
Connectivity
DCM
EEG
Network
Perceptual learning

ABSTRACT

The suppression of neuronal responses to a repeated event is a ubiquitous phenomenon in neuroscience. However, the underlying mechanisms remain largely unexplored. The aim of this study was to examine the temporal evolution of experience-dependent changes in connectivity induced by repeated stimuli. We recorded event-related potentials (ERPs) during frequency changes of a repeating tone. Bayesian inversion of dynamic causal models (DCM) of ERPs revealed systematic repetition-dependent changes in both intrinsic and extrinsic connections, within a hierarchical cortical network. Critically, these changes occurred very quickly, over inter-stimulus intervals that implicate short-term synaptic plasticity. Furthermore, intrinsic (within-source) connections showed biphasic changes that were much faster than changes in extrinsic (between-source) connections, which decreased monotonically with repetition. This study shows that auditory perceptual learning is associated with repetition-dependent plasticity in the human brain. It is remarkable that distinct changes in intrinsic and extrinsic connections could be quantified so reliably and non-invasively using EEG.

Introduction

We have previously used the roving paradigm and dynamic casual modelling (DCM) to search for optimum functional architectures underlying mismatch responses elicited by deviant and standard tones (Garrido et al., 2008). We were able to show that one can account for these responses with changes in connectivity among distributed cortical sources. In this paper, we adopt a parametric DCM to examine the form of repetition-dependent connectivity changes that mediate the emergence of these response differences. In brief, we attempt to model plasticity or changes in connectivity as a function of repetition or time. With this new approach we were able to quantify the time course of repetition-dependent changes and show that connectivity reduces, both within and between cortical areas. This causes decreases in evoked responses; *i.e.*, repetition suppression, which manifests as a suppression of a mismatch responses, as an oddball becomes a standard. A key practical advance, afforded by this parametric DCM, is the ability to quantify the rate of experience-dependent plasticity non-invasively, using simple and established paradigms. Furthermore, because we use a physiologically informed model, one can assess plasticity separately in intrinsic and extrinsic connections. This may be useful in clinical and neuropharmacological studies.

Novel events, or oddballs, embedded in a stream of repeated events, or standards, produce a distinct response that can be recorded non-invasively with electroencephalography (EEG). For example, the mismatch negativity (MMN) is the negative component of the waveform obtained by subtracting the event-related response to a standard from the response to an oddball, or deviant event. The MMN is believed to index an automatic change detection by pre-attentive sensory memory mechanisms (Tiitinen et al., 1994). Recently, we provided evidence that the mechanisms underlying the MMN can be considered within a hierarchical inference or predictive coding framework (Garrido et al., 2007a,b). Within this account, the MMN is interpreted as a failure to suppress prediction error, which can be explained quantitatively in terms of coupling changes among and within cortical regions. The predictive coding framework accommodates two previous hypotheses; in the sense that it predicts the adjustment of a perceptual model of the current stimulus [*c.f., the model-adjustment hypothesis* (Winkler et al., 1996; Näätänen and Winkler, 1999)] and entails adaptive changes in post-synaptic sensitivity during learning [*c.f., the adaptation hypothesis* (May et al., 1999; Jääskeläinen et al., 2004)]. The model-adjustment hypothesis postulates that the MMN reflects on-line modifications of a perceptual model that is updated when the auditory input does not match model predictions. In this context, the MMN is regarded as a marker for error detection, caused by a deviation from a learned regularity. In other words, the MMN is a response to an unexpected stimulus change and, from the point of view of predictive coding, signals prediction error.

* Corresponding author. UCLA Department of Psychology, 1285 Franz Hall, Box 951563, Los Angeles, CA 90095-1563, USA.
E-mail address: migarrido@ucla.edu (M.I. Garrido).

1053-8119/$ – see front matter © 2009 Elsevier Inc. All rights reserved.
doi:10.1016/j.neuroimage.2009.06.034

The mechanisms underlying suppression of prediction error are closely related to repetition suppression, in which "repeated experience with the same visual stimulus leads to both short and long-term suppression of neuronal responses in subpopulations of visual neurons" (Desimone, 1996). This is closely related to stimulus-specific adaptation (Pérez-González et al., 2005) in the auditory system, where "fast, highly stimulus-specific adaptation and slower plastic mechanisms work together to constantly adjust neuronal response properties to the statistics of the auditory scene" (Nelken, 2004). Repetition suppression is a ubiquitous phenomenon that speaks to both predictive coding (*e.g.*, Friston, 2005) and models of perceptual inference and learning (*e.g.*, Desimone, 1998). Predictive coding models of perceptual inference and learning suggest that all experience-dependent effects, and in particular repetition effects (from post-synaptic adaptation to semantic priming), are mediated by changes in synaptic efficacy; either short or long-term. These changes are driven by associative plasticity to optimise predictions of sensory input and therefore explain away prediction errors more efficiently. This enhanced 'explaining away' may be a useful perspective on repetition suppression, which rests on synaptic plasticity at the cellular level or changes in ensemble coupling at the macroscopic level. Critically, hierarchical inference, or predictive coding, also rests on optimising the relative influence of bottom-up prediction error and top-down predictions. This involves optimising the efficacy of intrinsic connections within an area or source (Friston, 2008). Put simply, when an unpredictable stimulus occurs, units encoding prediction error should adapt, reducing the strength of unreliable prediction error signals. In short, hierarchical inference, using prediction error, provides a principled framework in which the model adjustment and adaptation heuristics become necessary for understanding sensory inference (see Garrido et al., 2009a).

Few studies have explicitly explored the role of stimulus repetition during auditory memory-trace formation. Näätänen and Rinne (2002) found that later negative responses (>100 ms), in contrast to earlier responses, are elicited only by sound repetition. Others found that increasing the number of repetitions enhances responses to standard tones in both early (30–50 ms) and later components (60–75 ms) (Dyson et al., 2005), localised in the primary and secondary auditory areas respectively (Liegeois-Chauvel et al., 1994). Similarly, Baldeweg et al. (2004) and Haenschel et al. (2005) found that the MMN increases with the number of preceding standards and may be mediated by a repetition-dependent enhancement of a slow positive wave (50–250 ms) in the standard ERP (a repetition positivity — RP). In other words, the emergence of repetition positivity in standards underlies the mismatch negativity observed in a subsequent oddball.

Here we used a roving paradigm to test the hypothesis that repetition-dependent changes in electrophysiological responses to repeated stimuli are due to experience-dependent plasticity, or changes in connectivity. We show that stimulus repetition reduces connectivity, within and between cortical areas. This causes experience-dependent decreases in evoked responses; *i.e.*, repetition suppression, which manifests as a suppression of MMN components, as an oddball becomes sufficiently predictable to be considered as a standard.

Materials and methods

Subjects and stimuli

We studied ten healthy volunteers aged 24 to 34 (four females). Each subject gave signed informed consent before the study, which proceeded

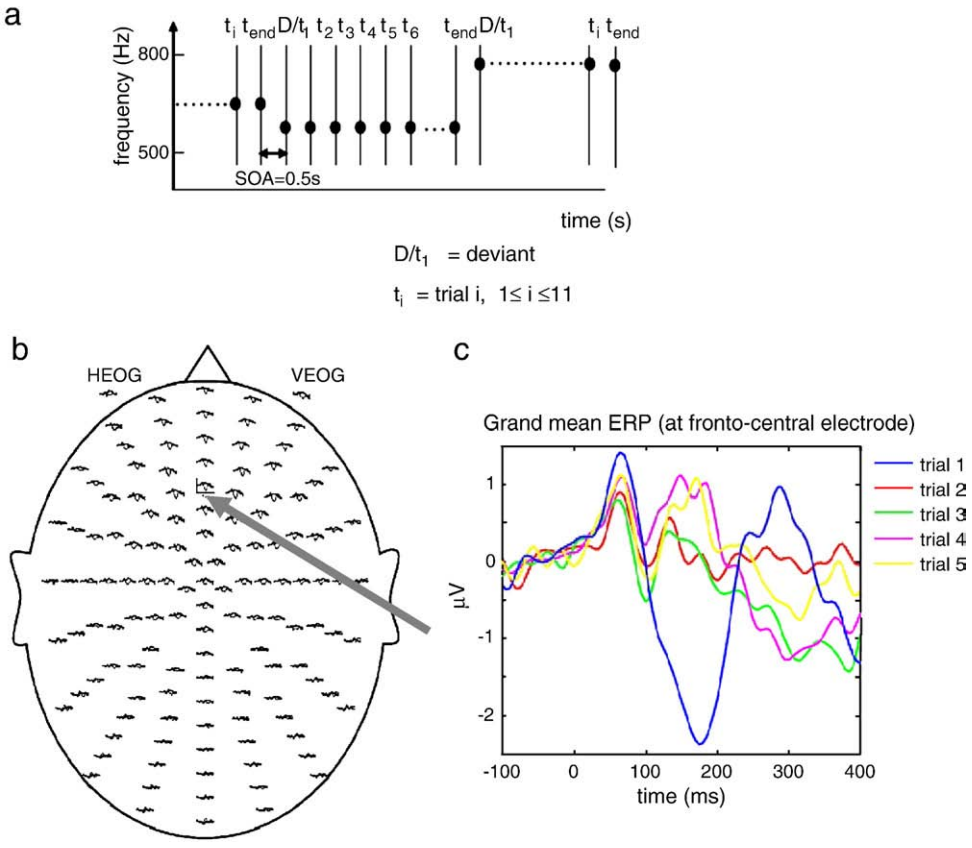

Fig. 1. Design and responses elicited in a roving paradigm. (a) The stimulus design is characterised by a sporadically changing standard stimulus. The first presentation of a novel tone is a *deviant* $D = t_1$ that becomes a *standard*, through repetition; $t_2,\ldots,t_{end}$. In this paradigm, deviants and standard have exactly the same physical properties. (b) Grand-mean (averaged over subjects) ERP responses to the sixth tone presentation, the established "standard" (t_6 — black) and deviant tone (t_1 — gray) overlaid on a scalp-map of 128 EEG electrodes. (c) ERP responses to tones sorted by number of repetitions at channel C21 (fronto-central). Trial 1 corresponds to responses elicited by the first tone presentation, or oddball events. The MMN response peaks at about 180 ms from change onset. Trials 2 to 5 correspond to the second to fifth repetitions of the same tone.

under local ethical committee guidelines. Subjects sat in front of a desk in a dimly illuminated room. Electroencephalographic activity was measured during an auditory roving 'oddball' paradigm (see Fig. 1a). The stimuli comprised a structured sequence of pure sinusoidal tones, with a roving, or sporadically changing tone. This paradigm entailed a few modifications to that used in Haenschel et al. (2005), originally from Cowan et al. (1993). Within each stimulus train, all tones were of one frequency and were followed by a train of a different frequency. The first tone of a train (*i.e.*, a tone with a different frequency from the preceding tone) was defined as a deviant. This deviant became a standard after few repetitions, as shown in Figs. 1 and 6 (see below). The ERP traces (Fig. 1) and the reconstructed sources (Fig. 6), reveal that by the third time a tone is presented, the evoked responses are very similar to those produced by subsequent tones, with no discernable difference between the fifth and further repetitions. In what follows, we will consider a standard to be the fifth (or subsequent) presentation of a tone.

This design means that deviants and standards have exactly the same physical properties; differing only in the number of times they have been presented. The number of times the same tone was presented varied randomly between one and eleven. The reason we presented runs of six or more tones was to ensure the subjects did not learn high-order regularities (*e.g.*, start to anticipate a change). Each subject was presented with ~245 deviant trials, ~235 first repetitions, ~230 second repetitions, ~220 third repetitions and ~210 fourth repetitions. The frequency of the tones varied from 500 to 800 Hz in 50 Hz intervals (*i.e.*, new tones were selected randomly from 500, 550, 600, 650, 700, 750, and 800 Hz). Stimuli were presented binaurally via headphones for 15 min. The duration of each tone was 70 ms, with 5 ms rise and fall times. The inter-stimulus interval was 500 ms: We chose this inter-stimulus interval to ensure that simple presynaptic facilitation could not explain any short-term plasticity observed. Short-term facilitation is a widely observed form of synaptic enhancement with a time course of about 200 ms. Multiunit recordings in cats suggest that "auditory cortical cells apparently have much faster recovery mechanisms than visual cortical cells". For example, findings based on models of presynaptic facilitation and depression suggest that auditory units have substantially shorter depression time constants (20 ms) than visual units (300 ms) and that facilitation decays with a time-constant of 60 ms (Eggermont, 1999). Presynaptic (calcium) mechanisms have been implicated in this process (Atluri and Regehr, 1996) and we wanted to ensure that any experience-dependant short-term plasticity observed was, at least in part, mediated by associative post-synaptic changes.

Each subject adjusted the loudness of the tones to a comfortable level, which was maintained throughout the experiment. The subjects performed an incidental visual task and were told to ignore the sounds. The task required a button-press whenever a fixation cross changed its luminance. This occurred randomly every 2 to 5 s (and did not coincide with auditory changes). We used an incidental visual task to suppress attention to the auditory stimuli and maintain attentional set. As anticipated, the P3a component of responses to oddballs was reduced in this paradigm (relative to attending the auditory stimulus; Garrido et al., 2007a), although not eliminated completely (data not shown).

Data acquisition and pre-processing

EEG was recorded with a *Biosemi* system (manufacturer) from 128 scalp electrodes at a sampling rate of 512 Hz. Vertical and horizontal eye movements were monitored using EOG (electro-oculograms) electrodes. Pre-processing and data analysis were performed within SPM5 (http://www.fil.ion.ucl.ac.uk/spm). The data were epoched offline, with a peristimulus window of −100 to 400 ms, down-sampled to 200 Hz, band-pass filtered between 0.5 and 40 Hz and re-referenced to the nose. Artefact removal was implemented with robust averaging. Robust averaging is a standard iterative scheme that produces the best estimate of the average by weighting data points as a function of their distance from the sample mean (*c.f.* Wager et al., 2005). Robust averaging will find the best average of each condition at every time point. This method gives a larger weight to points closer to the sample mean. Therefore, it has the advantage of taking into account all trials, while down-weighting outliers. Trials were sorted in terms of tone repetition. In other words, trials one to eleven correspond to the responses elicited after one to eleven presentations of the same tone, collapsed across the whole range of frequencies. Trial one is the oddball, or deviant trial.

For computational expediency, DCMs (see below) were computed on a reduced form of data. Instead of using the data from 128 channels, we performed a spatial reduction of these data and used its eight principal components, or spatial modes, as input for the DCM. These were the eight principal components of the covariance induced by varying the spatial parameters of the model. Two subjects were excluded from the DCM analysis due to an undetectable MMN (on visual inspection of the scalp data). Omitting these subjects may not seem good practice from the point of view of conventional ERP research. However, it can be motivated here by noting we were not trying to establish consistent mismatch responses over subjects; we were trying to characterise their time course, conditional on these responses being expressed.

Dynamic causal modelling

Dynamic causal model (DCM) was originally developed for connectivity analysis of fMRI (Friston et al., 2003) and subsequently EEG data (David et al., 2006a). DCMs for ERPs are spatiotemporal dipole models (Scherg and Van Cramon, 1985), which use a conventional formulation of source activity (*c.f.* equivalent current dipole or ECD models; Kiebel et al., 2006) but place constraints on the way signals are generated. These constraints require plausible neuronal interactions and rest on neural mass models (David et al., 2006b). Most approaches to connectivity analysis of M/EEG data use functional connectivity measures such as coherence or temporal correlations, which establish statistical dependencies between two time-series. However, there are many cases where causal interactions are of interest. In these situations, DCM has proven to be particularly useful, because it estimates effective connectivity (the influence one neuronal system has over another). DCM therefore provides an account of the interactions among cortical regions and allows one to make inferences about the connectivity parameters of a network; and how these parameters are influenced by experimental factors. DCM represents an important advance over conventional analyses of evoked responses because it places temporal constraints on the inversion; namely, activity in one source has to be caused by activity in another. DCMs for M/EEG use neural mass models (David and Friston, 2003) to explain source activity in terms of the ensemble dynamics of interacting inhibitory and excitatory subpopulations of neurons, based on the model of Jansen and Rit (1995). These subpopulations are interconnected according to the connectivity rules described in Felleman and Van Essen (1991) and furnish a hierarchical model of distributed electromagnetic sources in the brain.

A DCM for ERPs is specified in terms of its state equations and an observation model or output equation. The state equations for event-related potentials summarise average synaptic dynamics in terms of spike-rate-dependent current and voltage changes, for each subpopulation in the model

$$\dot{x} = f(x, u, \theta) \tag{1}$$

This means that the evolution of the neuronal states, x, is a function (parameterised by θ) of the states and experimental input u. The output equation couples specific states (the average depolarisation of pyramidal cells in each source $-x_0$) to the EEG signals y using a conventional linear electromagnetic forward model.

$$y = L(\theta)x_0 + \varepsilon \tag{2}$$

The lead field matrix, $L(\theta)$, (*i.e.*, the electromagnetic forward model) is parameterised in terms of the location and orientation of each source as described in Kiebel et al. (2006) and encodes the contribution of each source to the signal measured by scalp electrodes.

Eq. (1) summarises the state equations, specifying the rate of change of potentials and currents in one subpopulation as a function of currents and potentials in others (see Jansen and Rit, 1995; David et al., 2005, 2006a,b; and David and Friston, 2003 for further details). The state equations embody the model of connectivity and synaptic kinetics; where $\theta \supset \{C,\gamma,H,\tau\}$ includes extrinsic coupling parameters (forward, backward and lateral connections: $C_i : i = F,B,L$), intrinsic coupling parameters ($\gamma_i : i = 1,\ldots,4$), synaptic parameters ($H$ and τ), parameters of the experimental input function and conduction delays. We model each source with three subpopulations using the following state-equations

$$\begin{aligned}
\dot{x}_7 &= x_8 \\
\dot{x}_8 &= \frac{H_e}{\tau_e}((C_B + C_L + \gamma_3 I)S(x_0)) - \frac{2x_8}{\tau_e} - \frac{x_7}{\tau_e^2} \\
\dot{x}_1 &= x_4 \\
\dot{x}_4 &= \frac{H_e}{\tau_e}\left((C_F + C_L + \gamma_1 I)S(x_0) + C^U u\right) - \frac{2x_4}{\tau_e} - \frac{x_1}{\tau_e^2} \\
\dot{x}_0 &= x_5 - x_6 \\
\dot{x}_2 &= x_5 \\
\dot{x}_5 &= \frac{H_e}{\tau_e}((C_B + C_L)S(x_0) + \gamma_2 S(x_1)) - \frac{2x_5}{\tau_e} - \frac{x_2}{\tau_e^2} \\
\dot{x}_3 &= x_6 \\
\dot{x}_6 &= \frac{H_i}{\tau_i}\gamma_4 S(x_7) - \frac{2x_6}{\tau_i} - \frac{x_3}{\tau_i^2}
\end{aligned} \tag{3}$$

Here $x_i : i = 1,\ldots,8$ are the mean transmembrane potentials and currents of three subpopulations. The synaptic parameters H_e and H_i control maximum post-synaptic potentials for excitatory and inhibitory synapses respectively; while τ_e and τ_i represent the corresponding rate constants.

These state equations are first-order differential equations and are based on a neural mass model of population dynamics, where each subpopulation responds to experimental $u(t)$ and extrinsic input $S(x_i)$ with damped oscillations. Here, $S(x_i)$ corresponds to a sigmoid firing-function of a column-vector of depolarisations over sources. Integration of these equations is used to create predicted responses as a function of the unknown parameters. This allows the parameters to be optimised in relation to observed responses. This sort of DCM has been validated extensively in previous studies in terms of the source model (David and Friston, 2003; David et al., 2004, 2006a, 2006b; Kiebel et al., 2006; Moran et al., 2007, 2008), in the context of deep brain stimulation and epilepsy (David, 2007; David et al., 2008), and in the specific context used here (Garrido et al., 2007a,b, 2008, 2009b).

Model specification

Our network architectures were motivated by previous studies of MMN generators (Rinne et al., 2000; Opitz et al., 2002; Doeller et al., 2003; Grau et al., 2007; Garrido et al., 2007a,b, 2008, 2009b). These studies suggest bilateral sources located in the auditory cortex (*A1*), superior temporal gyrus (*STG*), and inferior frontal gyrus, which are usually stronger and found more consistently in the right hemisphere. In this study, we ignored putative frontal sources to focus on plasticity in symmetrically deployed auditory and temporal sources. Strictly speaking, we should have included a right frontal source in the DCM, given our previous model comparisons (Garrido et al., 2008, 2009b). However, we wanted to impose symmetry constraints on changes in coupling (to ensure precise estimates) and therefore used the best symmetrical architecture. In principle, it would be possible to use asymmetric models and Bayesian model comparison to justify this constraint but this is beyond the focus of the current paper.

DCM tries to explain differences among ERPs in terms of changes in specific coupling parameters. We chose to model the first five presentations because there was no discernable difference between the fourth and fifth (see Figs. 1 and 5) and there were fewer instances (*i.e.*, trials) of five or more repetitions. For the spatial model we used a three concentric sphere head model with homogeneous and isotropic conductivity as an approximation to the brain, cerebrospinal fluid, skull and scalp. The lead-field mapping cortical dipoles to channels was computed using the electromagnetic forward model solutions in the fieldtrip software (http://www2.ru.nl/fcdonders/fieldtrip). The coordinates reported by Opitz et al. (2002) for STG, and by Rademacher et al. (2001) for A1, were chosen as prior source location means. We converted these coordinates, given in the literature in Talairach space, to MNI space (http://imaging.mrc-cbu.cam.ac.uk/imaging/MniTalairach) (see Fig. 3). In all our models extrinsic connections were reciprocal and the experimental (subcortical auditory) input entered bilaterally through primary auditory sources.

Model inversion and inference

Statistical analyses in this paper were based on model comparison at the within and between-subject level. For within-subject DCM analyses, model m is inverted or fitted by optimising the parameters with respect to a variational free-energy bound on the model-evidence. This provides the conditional density of the model parameters, $p(\theta|y,m)$, and the models evidence, $p(y|m)$, for model comparison. Specifically, inversion of a DCM corresponds to approximating the posterior probability of the parameters using variational Bayes as described in Friston (2002). The aim is to minimise a free-energy bound on the log-evidence, with respect to a variational density, $q(\theta)$. After convergence the variational density is used as an approximation to the desired conditional density and the free-energy as an approximation to the log-evidence. The best model, given the data, is the one with highest log-evidence $\ln p(y|m)$ (assuming a uniform prior over models). Given two models m_1 and m_2 one can compare them through their Bayes factor (Penny et al., 2004) or, equivalently, the relative log-evidence; $\ln p(y|m_1) - \ln p(y|m_2)$. A difference in log-evidence of about three is considered strong evidence in favour of the more likely model. This is because a difference in log-evidence of three means the evidence for the more likely model is about twenty times the evidence for the other (http://en.wikipedia.org/wiki/Bayes_factors). At the between-subject level, we used classical inference (one-sample *t*-tests) on key parameters (encoding the parametric changes in connections with repetition). These parameters were summarised with their conditional expectation for each subject (*i.e.*, the mode or most likely value from the conditional density of each subject-specific DCM). This is known as the summary-statistic approach to random effects models.

Results

Our analysis comprised two parts: (i) confirmation that there is a significant response difference between the first and subsequent presentations of a tone and (ii) analysis of the plasticity in terms of coupling parameters that are a function of tone repetition.

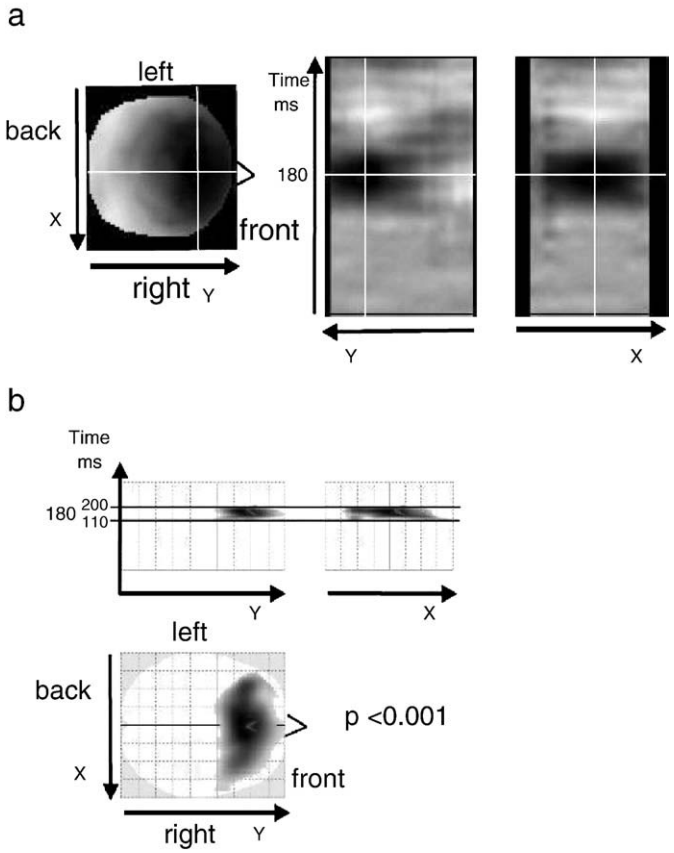

Fig. 2. 3D-spatiotemporal SPM analysis of the grand-mean difference at the between-subject level. The measurement space corresponds to a 2D-scalp topography (interpolated from the 128 channels) and peristimulus time (−100 to 400 ms). (a) Differential response with a negative peak at about 180 ms. (b) SPM showing regions where there is a significant negativity in the difference ($p<0.001$ uncorrected). Significant effects were found over temporal and frontal areas in the range of 110 to 200 ms peaking at 180 ms (see marker).

Repetition effects

An initial sensor-space analysis was performed to confirm the presence of a repetition-dependent response in our roving paradigm. For these analyses, the channel data were transformed into scalp-map images (see Fig. 2a). These were obtained after linear interpolation and smoothing (at FWHM 6 mm×6 mm×20 ms) of the difference wave between the first presentation and the sixth presentation (*i.e.*, fifth repetition). Fig. 1b (gray) shows the grand-mean responses (over subjects) to the first tone at a fronto-central electrode (C21). This corresponds to the oddball response. The responses to the fifth repetition (black) correspond to the learned or "standard" response. The responses to the fifth repetition are very similar to those elicited by standards in conventional oddball paradigms (see also Garrido et al., 2007a). A mismatch response was found over the frontal and central electrodes, peaking at about 180 ms from change onset, which is consistent with previous studies (Baldeweg et al., 2004; Cowan et al., 1993). Critically, these response differences cannot be explained by differences in stimuli *per se*, because the first and sixth stimuli were physically identical; this is one of the powerful aspects of the roving paradigm. Fig. 1c shows responses to tones sorted by number of repetitions at channel C21 (fronto-central). Trial 1 corresponds to responses elicited by the first tone presentation, or oddball events and trials 2 to 5 correspond to the first to fourth repetitions of the same tone. It can be seen that the MMN is diminished substantially after the second presentation.

Fig. 2 shows a 3D-spatiotemporal characterisation of the grand-mean responses, using statistical parametric mapping to compare the first and the sixth presentations; the "deviant" and the "standard", respectively. This analysis searched for differences over 2D sensor-space and all peristimulus times [−100, 400 ms]. The scalp topography at each time-bin was interpolated from 128 channels and smoothed. Fig. 2a shows the intensity of the differential response and that its negative peak occurs at about 180 ms, over the frontal and central areas. Fig. 2b shows the corresponding statistical parametric map (SPM; displayed at $p<0.001$ uncorrected) showing where there is a significant negative difference over subjects. This SPM showed a significant MMN over temporal and frontal areas between 110 and 200 ms, with maximum at 180 ms.

Repetition-dependent plasticity — a parametric DCM

The aim of this study was to investigate the plasticity that explains the repetition effect above. A dynamic causal model (DCM; see Fig. 3) was used to explain differences among ERPs in terms of parametric changes in coupling. Given the nature of repetition suppression in unit electrode recordings and experience with the roving paradigm, we expected that the connectivity would decrease as a function of repetition. However, we did not want to constrain the rate or form of this decrease and therefore modelled these effects with two temporal basis functions: a monotonic exponential decay, modelling slow cumulative effects and a phasic function peaking after the second tone. The choice of the particular basis functions is not particularly important, provided their linear

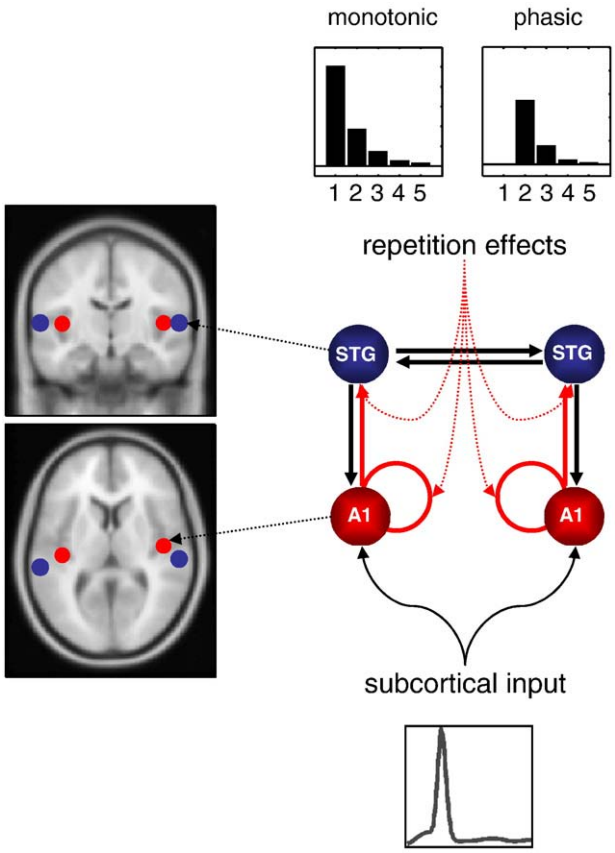

Fig. 3. Model specification: (Right) Sources comprising the networks: A1: primary auditory cortex, and STG: superior temporal gyrus are connected with forward (red), backward (black) and intrinsic (red) connections. (Left) Source locations: Their prior mean locations: left A1 [−42, −22, 7], right A1 [46, −14, 8], left STG [−61, −32, 8], right STG [59, −25, 8], in mm are superimposed in an MRI of a standard brain in Montreal Neurological Institute space. The DCM receives (parameterised) subcortical input at the A1 sources, which elicit transient perturbations in the remaining sources. Plasticity is modelled by changes in intrinsic and forward connections (red) that are a mixture of monotonic (upper left) and phasic (upper right) repetition-specific effects.

combinations can cover all plausible time-courses one might expect to see. The first modelled the evolution of connection strength as an exponential function of tone repetition, $r = 0,\ldots 4$.

$$E(r) = \exp(-r) \tag{4}$$

The second was a phasic (gamma-density) function, which peaked after the first tone:

$$G(r) = \frac{4r\exp(-2r)}{\Gamma(2)} \tag{5}$$

Using these parametric forms, we inverted two DCMs, corresponding to two competing hypotheses: (i) that tone repetition causes a monotonic decrease in connection strengths (E — using just the exponential basis function), and (ii) that tone repetition causes 'one-shot' or changes in coupling (EG — using both basis functions). This more flexible model used a mixture of both parametric effects (see Fig. 3; upper panels). The two DCMs were tested against a naïve or null model that precluded connectivity changes. The network used for these analyses is shown in Fig. 3 and comprised two low-level (auditory) sources, one in each hemisphere, and two high-level (temporal) sources. We modelled repetition-dependent changes in forward connections (from the auditory sources) and intrinsic connections (within the auditory sources), allowing for separate repetition-dependent (symmetrical) modulation of extrinsic and intrinsic connections. The adaptation hypothesis (Jääskeläinen et al., 2004) postulates that the MMN arises predominantly from synaptic adaptation (*c.f.* May et al., 1999). Here, we model these effects through changes in intrinsic connectivity, modelled by source-specific post-synaptic density parameters (see Kiebel et al., 2007 for details). These effects could be mediated by adaptation [*e.g.*, due to increase in calcium-dependent potassium conductances, leading to after-hyperpolarizing currents (Powers et al., 1999) or subsequent calcium-dependent intracellular mechanisms that underlie phenomena like paired-pulse depression (*e.g.* Davies et al., 1990). From a functional perspective, putative short-term changes in the synaptic efficacy of intrinsic afferents modify lateral interactions within primary auditory cortex. In the predictive coding framework, these encode the precision of prediction errors. Similar changes in extrinsic

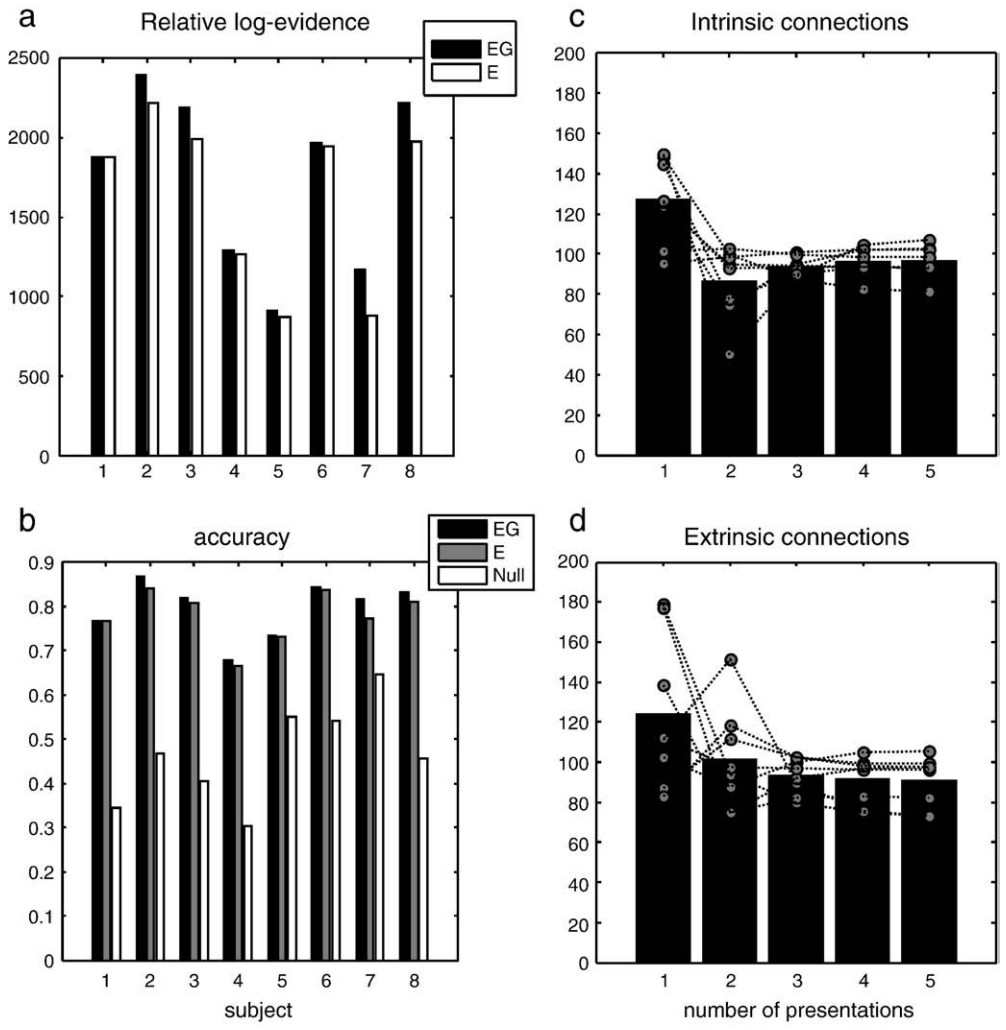

Fig. 4. Model comparisons and conditional expectations for repetition-dependent connectivity changes. (a) Bayesian model comparison shows that model EG supervenes over model E in seven out of eight subjects; data from the first subject were best explained by the exponential (monotonic) model but this effect was trivial in relation to the log-evidence in relation to the null model. (b) Corresponding results for model accuracy expressed in terms of the proportion of variance explained by the model (*i.e.*, the coefficient of determination). (c) Connectivity changes with repetition. This shows the temporal evolution of connectivity as a function of time, or repetition for the intrinsic connections within A1, expressed as the average conditional expectation over subjects (bars) and for each subject separately (circles). These repetition effects are normalised so that the connection strength is a percentage of average strength over trials. There is a very consistent and marked decrease in coupling after the first presentation that appears to rebound on subsequent presentations. (d) The same results for the extrinsic connections. Here the changes are expressed more slowly as a function of repetition, exhibiting, on average, a monotonic decrease over time.

(forward connections) correspond to perceptual learning or model adjustment (see Winkler et al., 1996; Näätänen and Winkler, 1999; Friston, 2005).

Bayesian model comparison revealed that the EG model supervened over the simple monotonic model E, in all but one subject; and in all subjects both parametric models were substantially better than the null model that precluded plasticity. This means that there is consistent and strong evidence for changes in connectivity, above and beyond a simple exponential decay, in one or more connections (see Fig. 4a). Fig. 4b shows the equivalent results for model accuracy

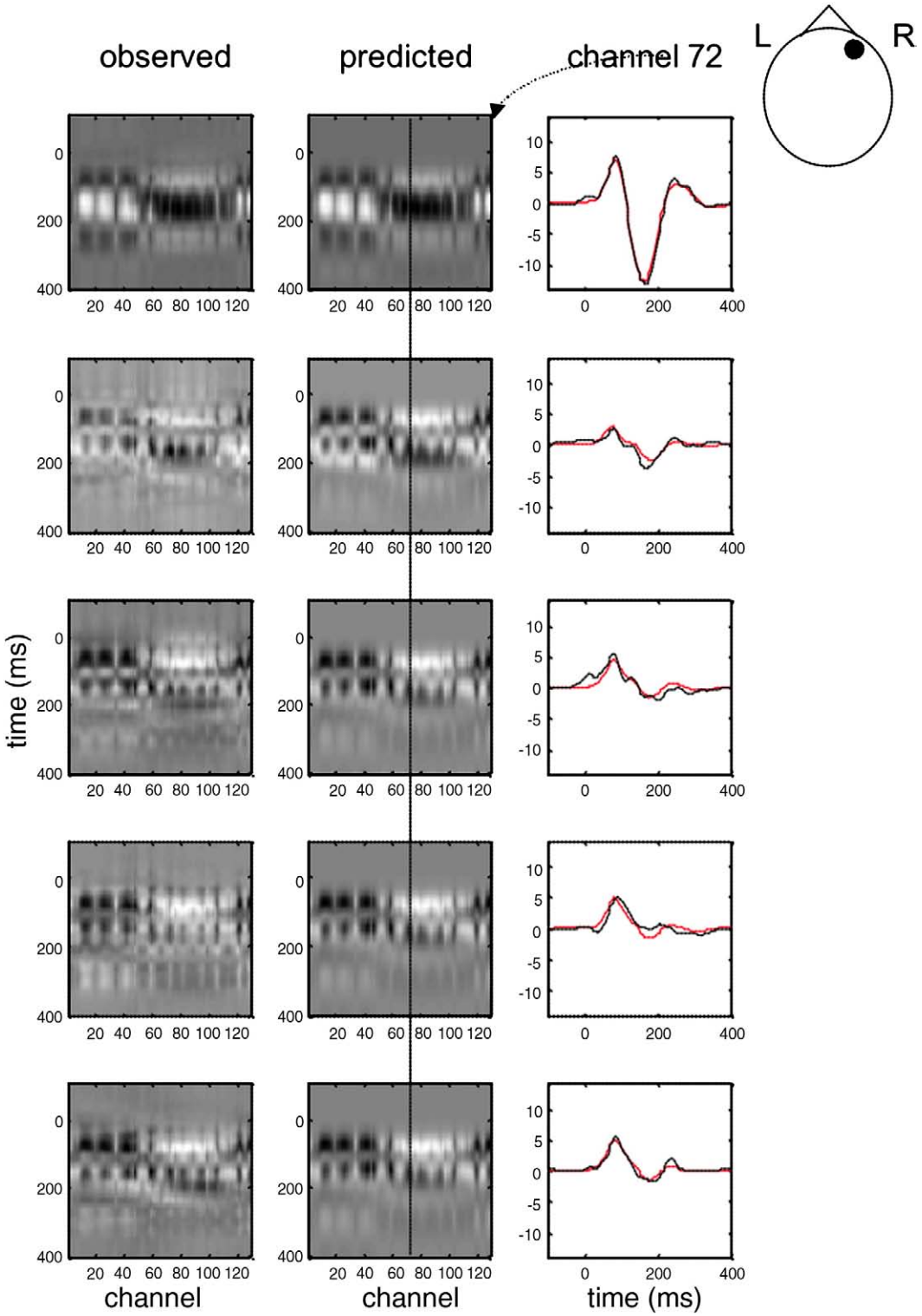

Fig. 5. Predicted and observed responses in channel space. Responses were averaged over all subjects (Hanning window from −100 ms to 400 ms): (left) image format responses over peristimulus time and channels for each of the five repetitions. Profound mismatch negativity is seen in the upper panels (first presentation) that disappear quickly to produce the standard response by the fifth presentation. (right column). The predicted (red) and observed (black) responses for channel 72 are shown on the right for illustration. The agreement is self-evident. Responses to repeating tones show a decrease in the N1 component (peaking at about 100 ms) and later in the MMN, which vanishes after two repetitions.

expressed as the proportion of variance explained over channels and trials by each of the three models assessed. (The EG model explained 80% of variance on average and at least 68% in each subject.)

Fig. 4 also shows the changes in coupling strengths of the intrinsic (Fig. 4c) and extrinsic (Fig. 4d) connections. Here, the evolution of connectivity is shown as a function of repetition in terms of conditional expectations from the DCM analyses. These results suggest that auditory learning involves a rapid decrease and subsequent rebound in *intrinsic* connections and a slow monotonic decrease in *extrinsic* connections. These parameter estimates encode repetition-dependent changes in effective connectivity. In this (biophysical) DCM, effective connectivity parameterises synaptic connectivity; therefore, these changes can be regarded as an estimate of plasticity.

The bars represent the average (across subjects) of the estimated intrinsic coupling parameters within A1 (Fig. 4c) and the extrinsic forward connections linking A1 with the ipsilateral STG (Fig. 4d). Both are normalised to the average coupling strength. Intrinsic connections show a massive (~30%) decrease after the first presentation; this is seen in all but two subjects. Critically, in all but two subjects, there is a rebound in intrinsic connectivity on the third presentation. This biphasic plasticity was modelled by a large positive exponential component and a large negative gamma component. These two parametric effects were significant over subjects ($t=3.49$, $df=7$; $p=0.0051$ and $t=2.08$, $df=7$; $p=0.0379$ respectively). On the other hand, forward connections showed a slower decay with stimulus repetition that was monotonic. In this instance, only the exponential component was significant over subjects ($t=2.01$, $df=7$; $p=0.0422$), whereas the biphasic gamma component showed no consistent contribution ($t=0.04$, $df=7$; $p=0.4832$).

Fig. 5 shows the observed and predicted responses elicited by the first five tones (the oddball trial and subsequent repetitions). These are shown over channels and peristimulus time in image format (left and middle columns) and for a representative electrode (right columns). These data are the summed responses over all subjects (after applying a Hanning window that suppresses variations early and late in peristimulus time). The response to the first presentation or oddball shows a peak after 100 ms (that subtends the N1 component) and an enhanced response with its maximum at about 180 ms. Visual inspection of the scalp data (not shown) suggested that the later peak conforms to the spatial deployment of the MMN. The second and subsequent presentations elicit a response with a similar temporal profile, but the MMN component is greatly attenuated. This suggests that, after one presentation of a new tone, the brain has re-learned the auditory context; in other words, the "standard" is largely learned (*c.f.* Baldeweg et al., 2004; Dyson et al., 2005; Haenschel et al., 2005). Fig. 6 shows the reconstructed responses (summed over subjects) at the source level for bilateral primary auditory cortex (A1)

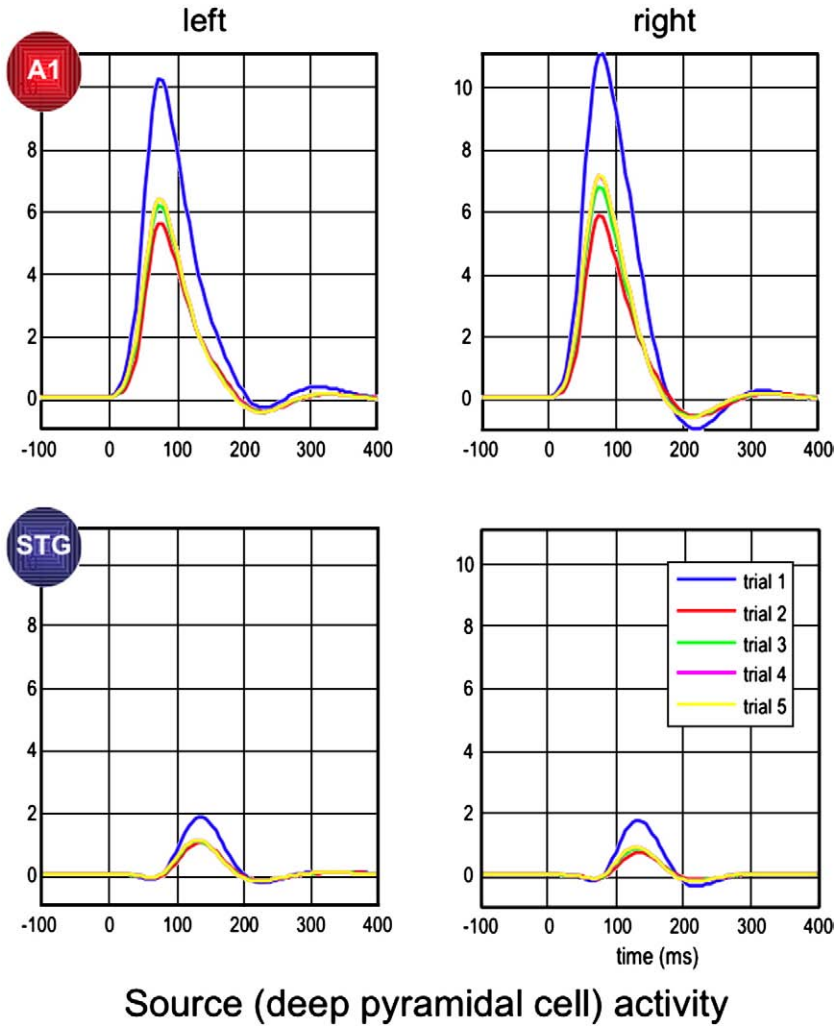

Fig. 6. Reconstructed responses in bilateral primary auditory cortex (upper panels) and bilateral superior temporal gyrus (lower panels). These are the source reconstructed averages over subjects. The five trials correspond to repetitions of the same event. Right and left A1 and show peak activities at about 80 ms that are suppressed to about half their amplitude after the first presentation; indeed it is suppressed so much that it recovers slightly on subsequent presentations. In bilateral STG, peak activity is observed at about 140 ms, with the greatest amplitude on the first presentation.

and bilateral superior temporal gyrus (STG). The generators for the N1 component lie in A1 but not at the level of STG. Activity peaking between 100 and 200 ms is seen in STG that might underlie the MMN. This spatiotemporal dissociation of N1 and MMN generators is very reminiscent of the findings in Jääskeläinen et al. (2004). These source-level responses show the complicated hierarchical changes in the ERP with repetition; in low-level auditory sources the first repetition evokes a greater response during the N1, which is suppressed profoundly on the first repetition. It then recovers to the level of the oddball response with subsequent repetitions. Conversely, in higher (superior temporal) sources, the first repetition produces a later response (that shapes later A1 activity through backward connections — see Fig. 6, upper panels). This again is suppressed on repetition, but with no rebound. All these effects are explained by a rapid biphasic change in intrinsic connectivity and more persistent monotonic changes in extrinsic connectivity.

Discussion

In summary, this study presents the first attempt to quantify plasticity underlying sensory memory formation, caused by stimulus repetition with a network of interacting cortical sources using EEG. We investigated the effect of stimulus repetition on scalp electroencephalographic responses and studied the underlying dynamics of the cortical network that generates these responses. Subjects were presented with a roving paradigm, a modified auditory oddball paradigm with tones that change sporadically to another frequency. Deviant tones elicited an MMN response peaking at about 180 ms over fronto-central channels (see Figs. 1 and 2). The difference wave between responses to deviants and responses to standards (here assumed to be established after the fifth repetition) revealed a statistically significant negativity between 110 and 200 ms (Fig. 2b). This result is consistent with previous findings (Sams et al., 1985; Näätänen and Rinne, 2002; Baldeweg et al., 2004). Note that standards and deviants, as defined here, are physically identical; therefore, the MMN cannot be due to different responses in frequency-specific auditory neurons but to experience-dependent changes in the same neuronal subpopulations. The MMN was explained by changes in the strength of the connectivity within and between the cortical sources of the underlying network (see Figs. 3 and 4).

This is the first analysis of ERPs, within the DCM framework, that uses parametric effects; all responses from the first to the fifth presentation were modelled simultaneously, using parameterised connectivity changes. Bayesian model comparison revealed that as the plasticity of the underlying cortical network unfolds, connection strengths show a progressive decrease with some connections exhibiting fast or biphasic changes (Fig. 4). Specifically, intrinsic connections within bilateral A1 show a fast depression, followed by a rebound, whereas forward connections show a slower decay. These results suggest that perceptual learning, caused by stimulus repetition, can be explained by plasticity in intrinsic (adaptation) and extrinsic (model learning) brain connections. An interesting finding is that the MMN vanishes after one or two repetitions (Fig. 5), suggesting that the brain learns the context established by auditory trains within a second or so. These findings accord with Liegeois-Chauvel et al. (1994) who found that the generators of early components are distributed along A1 and support the propagation hypothesis postulated by Baldeweg (2006): that a sensory memory trace can be detected earlier and earlier, at the level of A1, with an increasing number of repetitions. This is also consistent with the idea that stimulus-specific adaptation in A1 contributes to the emergence of the MMN (Ulanovsky et al., 2003); although our modelling suggests that stimulus-specific adaptation is expressed vicariously through later responses in secondary or higher temporal sources. The decrease in inter-regional connection strengths over repetitions is also consistent with predictive coding theories (Rao and Ballard, 1999; Friston, 2005; Baldeweg, 2006). From this perspective, within-trial changes correspond to perceptual inference, whereas between-trial changes correspond to perceptual learning.

Implications

We wanted to test the hypothesis that the MMN could be explained in terms of repetition suppression; a phenomenon originally studied in the visual system using unit electrode recordings (Desimone, 1998). In addition, we wanted to assess the relative contribution of plasticity in intrinsic (*i.e.*, adaptation) and extrinsic (*i.e.*, hierarchical learning) connectivity. We found, as anticipated, both exhibited repetition-dependent changes; however, the time-courses of these changes were distinct. The biphasic changes in intrinsic connections are especially interesting from a mechanistic perspective: One might assume that intrinsic connections should reflect stimulus-specific adaptation and should therefore show a monotonic decrease with repetition. However, an alternative perspective (Friston, 2008) suggests that intrinsic connectivity may reflect the estimated precision of prediction error, which should fall *after* the oddball and then recover with learning. This is what we found and suggests that changes in the synaptic efficacy of extrinsic and intrinsic connections may mediate stimulus-specific adaptation by encoding prediction errors and their precision respectively.

This finding speaks to distinct synaptic mechanisms. This is important, both from the perspective of computational theories of sensory learning and how these computations are implemented physiologically. The connection with paired-pulse paradigms used to study synaptic facilitation and depression (Davies et al., 1990) is self-evident (paired-pulse paradigms, by design, harness repetition suppression) and suggests that the relative time-scales of intrinsic and extrinsic plasticity could be characterised by varying the inter-stimulus interval in roving paradigms. Furthermore, combining this with pharmacological interventions is motivated easily by existing psychopharmacological studies of the MMN; see Baldeweg et al. (2004) for a discussion of these studies, in relation to schizophrenia research.

Modelling issues

This is the first time that we have used parametric DCM for ERPs to address plasticity: to maximise the probability of getting a significant result we focused on a simple question using a simple architecture; namely, could we find evidence for a difference in plasticity between intrinsic and extrinsic connections in a minimal symmetric model. We were pleased with the results and especially their consistency over subjects. However, this is a rather crude characterisation of the plasticity underlying stimulus-specific adaptation and repetition effects in the MMN paradigm. For example, we did not examine differences between forward and backward extrinsic connections or, critically, extrinsic connections at different hierarchical levels. We hope to examine these issues in future work using full hierarchical architectures (*e.g.*, including the inferior frontal source implicated by our previous model comparison work; Garrido et al., 2008, 2009b or possibly subcortical sources; Pérez-González et al., 2008).

The reason why we used a simple model is because adding regions (or plastic connections) increases the number of free parameters. This induces conditional correlations among the parameter estimates and an increase in their conditional variance. Practically, this increases inter-subject variability and makes it more difficult to establish consistent changes in coupling strength. The present model is as simple as we could make it: notice that both the intrinsic and extrinsic connections (that can change) are the same (*i.e.* intrinsic to A1 and forward from A1), enabling us to impose symmetry constraints and reduce the number of free parameters. This next stage will entail more

ambitious models that may speak to the hierarchical mechanisms that underpin ERP changes in the MMN paradigm.

We have already established, using this paradigm, that a hierarchical model with two pairs of bilateral sources is a much better model of the data than one pair of auditory sources (Garrido et al., 2008, 2009b). Conventional analyses localise sources associated with a specific peak and latency. In contrast, DCM explains a whole time-window, in this paper the −100 to 400 ms. Therefore, the models considered here attempt to explain the dynamics during that time interval, including the MMN and any other component peaking under these time limits, such as RP, N1 or P3a.

In DCM, the parameters (and models) are optimised in relation to their evidence; this is the probability of the data under a particular model. This means the parameter estimates (and model selection) depends on the data that are explained. In ERP research, this means that the choice of peristimulus time-window is critical. We have used this dependency previously to show that models with backward connections are needed to explain data that include later components (especially after 220 ms), relative to data that do not (Garrido et al., 2007b). In our previous study of the roving paradigm (Garrido et al., 2008) ERPs were modelled from 0 to 250 ms, whereas in this paper we used a time-window of −100 to 400 ms. Modelling a longer time interval is computationally demanding but obliges the model to explain more of the ERPs and their differences. We chose a relatively long time-window because the mechanisms we hypothesized for explaining stimulus-specific adaptation or repetition effects have time constants in the hundreds of milliseconds to seconds (*i.e.*, short-term changes in synaptic plasticity). This is because these changes have to persist over the inter-stimulus interval to mediate repetition suppression. The use of a long window precludes any interpretation in relation to the MMN *per se* because this is embedded in the ERP differences modelled. However, it does sensitize the analysis to the sorts of mechanisms that might underlie stimulus-specific adaptation in the MMN paradigm.

Note that our parametric DCM analysis attempted to explain the data caused by five successive tone presentations. Hence, the evidence pertains to the ERPs evoked over multiple stimulus conditions and their differences. Finally, it is important to note that DCM is a useful tool only if the model assumptions are satisfied and model specification is biologically well motivated; see David et al. (2006a) and Garrido et al. (2007a) for a thorough discussion of the limitations of DCM and the consequences of violating its assumptions.

The MMN, a marker for perceptual learning

The MMN is thought to reflect error detection and is caused by an unexpected or unlearnt event. This fits comfortably with theoretical suggestions that the MMN can be framed within hierarchical models of inference and learning that appeal to predictive coding (Friston, 2003, 2005; Baldeweg, 2006; Garrido et al., 2007a,b, 2008 2009b). In this paper, we show that learning through repetition leads to reduction of evoked responses and that these are associated with changes in connectivity within and between cortical sources. Suppression of evoked responses due to repeated events has been encountered in other domains; such as visual memory (Desimone, 1996), face perception and recognition (Henson et al., 2003) and in motor-learning (Friston et al., 1992). Our results suggest that learning regularities in the auditory environment involves changes of connectivity. This plasticity in extrinsic connections shows a slow exponential decay as a function of event repetition, probably reflecting reduction of surprise, as a novel event becomes predictable. In contrast, plasticity in intrinsic connections exhibits a fast decay followed by a slow rebound. This might reflect an initial decrease in the estimated precision of predictions, induced by the oddball, and then a gradual recovery with learning. In short, we have shown that the brain needs only a few repetitions to predict the next stimulus, and that this prediction may involve plastic changes within and between cortical regions (see also Ulanovsky et al., 2004; Pérez-González et al., 2008).

Conclusion

The key contribution of this work is to show that the plasticity underlying stimulus-specific adaptation and perceptual learning can occur very quickly and is effectively complete after a few presentations of a stimulus. Furthermore, the putative experience-dependent plasticity that underlies this learning (as observed electrophysiologically) involves distinct changes in intrinsic and extrinsic connections and, implicitly, distributed interactions among multiple sources. This study provides proof of principle that one can estimate changes in connectivity in the human brain using non-invasive, widely available techniques, in a matter of minutes and using a standard paradigm. This may be a useful way to quantify experience-dependent plasticity in distributed brain systems; not only in systems neuroscience but neuropsychiatric disorders that involve disconnection or abnormal plasticity.

Acknowledgments

We thank David Bradbury for technical support and the volunteers for participating in this study. We thank Russell Poldrack for helpful comments on the manuscript. This work was supported by the Portuguese Foundation for Science and Technology (SFRH/BD/13481/2003 to M.I.G.) and the Wellcome Trust.

All the software necessary to implement these analyses is available as part of the SPM academic freeware (http://www.fil.ion.ucl.ac.uk/spm).

References

Atluri, P.P., Regehr, W.G., 1996. Determinants of the time course of facilitation at the granule cell to Purkinje cell synapse. J. Neurosci. 16 (18), 5661–5671.
Baldeweg, T., 2006. Repetition effects to sounds: evidence for predictive coding in the auditory system. Trends Cogn. Sci. 10, 93–94.
Baldeweg, T., Klugman, A., Gruzelier, J., Hirsch, S.R., 2004. Mismatch negativity potentials and cognitive impairment in schizophrenia. Schizophr. Res. 69, 203–217.
Cowan, N., Winkler, I., Teder, W., Näätänen, R., 1993. Memory pre-requisites of mismatch negativity in the auditory even-related potential (ERP). J. Exp. Psychol. Learn. Mem. Cogn. 19, 909–921.
David, O., 2007. Dynamic causal models and autopoietic systems. Biol. Res. 40, 487–502.
David, O., Friston, K.J., 2003. A neural mass model for MEG/EEG: coupling and neuronal dynamics. NeuroImage 20, 743–1755.
David, O., Cosmelli, D., Friston, K.J., 2004. Evaluation of different measures of functional connectivity using a neural mass model. NeuroImage 21, 659–673.
David, O., Harrison, L., Friston, K.J., 2005. Modelling event-related responses in the brain. NeuroImage 25, 756–770.
David, O., Kiebel, S.J., Harrison, L.M., Mattout, J., Kilner, J.M., Friston, K.J., 2006a. Dynamic causal modelling of evoked responses in EEG and MEG. NeuroImage 30, 1255–1272.
David, O., Kilner, J.M., Friston, K.J., 2006b. Mechanisms of evoked and induced responses in MEG/EEG. NeuroImage 31, 1580–1591.
David, O., Woźniak, A., Minotti, L., Philippe, K., 2008. Preictal short-term plasticity induced by intracerebral 1 Hz stimulation. NeuroImage 39, 1633–1646.
Davies, C.H., Davies, S.N., Collingridge, G.L., 1990. Paired-pulse depression of monosynaptic GABA-mediated inhibitory postsynaptic responses in rat hippocampus. J. Physiol. 424, 513–531.
Desimone, R., 1996. Neural mechanisms for visual memory and their role in attention. Proc. Natl. Acad. Sci. U. S. A. 93, 13494–13499.
Desimone, R., 1998. Visual attention mediated by biased competition in extrastriate visual cortex. Philos. Trans. R. Soc. Lond., B Biol. Sci. 353, 1245–1255.
Doeller, C.F., Opitz, B., Mecklinger, A., Krick, C., Reith, W., Schröger, E., 2003. Prefrontal cortex involvement in preattentive auditory deviance detection: neuroimaging and electrophysiological evidence. NeuroImage 20, 1270–1282.
Dyson, B.J., Alain, C., He, Y., 2005. I've heard it all before: perceptual invariance represented by early cortical auditory-evoked responses. Brain Res. Cogn. Brain Res. 23, 457–460.
Eggermont, J.J., 1999. The magnitude and phase of temporal modulation transfer functions in cat auditory cortex. J. Neurosci. 19 (7), 2780–2788.
Felleman, D.J., Van Essen, D.C., 1991. Distributed hierarchical processing in the primate cerebral cortex. Cereb. Cortex 1, 1–47.
Friston, K.J., Frith, C.D., Passingham, R.E., Liddle, P.F., Frackowiak, R.S., 1992. Motor practice and neurophysiological adaptation in the cerebellum: a positron tomography study. Proc. Biol. Sci. 248, 223–228.

Friston, K.J., 2002. Bayesian estimation of dynamical systems: an application to fMRI. NeuroImage 16, 513–530.
Friston, K., 2003. Learning and inference in the brain. Neural Netw. 16, 1325–1352.
Friston, K., 2005. A theory of cortical responses. Philos. Trans. R. Soc. Lond., B. Biol. Sci. 360, 815–836.
Friston, K., 2008. Hierarchical models in the brain. PLoS Comput. Biol. 4 (11), e1000211.
Friston, K.J., Harrison, L., Penny, W., 2003. Dynamic causal modelling. NeuroImage 19, 1273–1302.
Garrido, M.I., Kilner, J.M., Kiebel, S.J., Stephan, K.E., Friston, K.J., 2007a. Dynamic causal modelling of evoked potentials: a reproducibility study. NeuroImage 36, 571–580.
Garrido, M.I., Kilner, J.M., Kiebel, Friston, K.J., 2007b. Evoked brain responses are generated by feedback loops. Proc. Natl. Acad. Sci. U. S. A. 104 (52), 20961–20966.
Garrido, M.I., Friston, K.J., Kiebel, S.J., Stephan, K.E., Baldeweg, T., Kilner, J.M., 2008. The functional anatomy of the MMN: a DCM study of the roving paradigm. NeuroImage 42, 936–944.
Garrido, M.I., Kilner, J.M., Stephan, K.E., Friston, K.J., 2009a. The mismatch negativity: a review of the underlying mechanisms. Clin. Neurophysiol. 120, 453–463.
Garrido, M.I., Kilner, J.M., Kiebel, S.J., Friston, K.J., 2009b. Dynamic causal modeling of the response to frequency deviants. J. Neurophysiol. 101, 2620–2631.
Grau, C., Fuentemilla, L.I., Marco-Pallares, J., 2007. Functional neural dynamics underlying auditory event-related N1 and N1 suppression response. NeuroImage 36, 522–531.
Haenschel, C., Vernon, D.J., Prabuddh, D., Gruzelier, J.H., Baldeweg, T., 2005. Event-related brain potential correlates of human auditory sensory memory-trace formation. J. Neurosci. 25, 10494–10501.
Henson, R.N., Goshen-Gottstein, Y., Ganel, T., Otten, L.J., Quayle, A., Rugg, M.D., 2003. Electrophysiological and haemodynamic correlates of face perception, recognition and priming. Cereb. Cortex 13, 793–805.
Jääskeläinen, I.P., Ahveninen, J., Bonmassar, G., Dale, A.M., Ilmoniemi, R.J., Levänen, S., Lin, F.H., May, P., Melcher, J., Stufflebeam, S., Tiitinen, H., Belliveau, J.W., 2004. Human posterior auditory cortex gates novel sounds to consciousness. Proc. Natl. Acad. Sci. U. S. A. 101, 6809–6814.
Jansen, B.H., Rit, V.G., 1995. Electroencephalogram and visual evoked potential generation in a mathematical model of coupled cortical columns. Biol. Cybern. 73, 357–366.
Kiebel, S.J., David, O., Friston, K.J., 2006. Dynamic causal modelling of evoked responses in EEG/MEG with lead field parameterization. NeuroImage 30, 1273–1284.
Kiebel, S.J., Garrido, M.I., Friston, K.J., 2007. Dynamic causal modelling of evoked responses: the role of intrinsic connections. NeuroImage 36, 332–345.
Liegeois-Chauvel, C., Musolino, A., Badier, J.M., Marquis, P., Chauvel, P., 1994. Evoked potentials recorded from the auditory cortex in the man: evaluation and topography of the middle latency components. Electroencephalogr. Clin. Neurophysiol. 92, 204–214.
May, P., Tiitinen, H., Ilmoniemi, R.J., Nyman, G., Taylor, J.G., Näätänen, R., 1999. Frequency change detection in human auditory cortex. J. Comput. Neurosci. 6, 99–120.
Moran, R.J., Kiebel, S.J., Stephan, K.E., Reilly, R.B., Daunizeau, J., Friston, K.J., 2007. A neural mass model of spectral responses in electrophysiology. NeuroImage 37, 706–720.
Moran, R.J., Stephan, K.E., Kiebel, S.J., Rombach, N., O'Connor, W.T., Murphy, K.J., Reilly, R.B., Friston, K.J., 2008. Bayesian estimation of synaptic physiology from the spectral responses of neural masses. NeuroImage 42, 272–284.
Näätänen, R., Rinne, T., 2002. Electric brain response to sound repetition in humans: an index of long-term-memory — trace formation? Neurosci. Lett. 318, 49–51.
Näätänen, R., Winkler, I., 1999. The concept of auditory stimulus representation in cognitive neuroscience. Psychol. Bull. 125, 826–859.
Nelken, I., 2004. Processing of complex stimuli and natural scenes in the auditory cortex. Curr. Opin. Neurobiol. 14 (4), 474–480.
Opitz, B., Rinne, T., Mecklinger, A., von Cramon, D.Y., Schröger, E., 2002. Differential contribution of frontal and temporal cortices to auditory change detection: fMRI and ERP results. NeuroImage 15, 167–174.
Penny, W.D., Stephan, K.E., Mechelli, A., Friston, K.J., 2004. Comparing dynamic causal models. NeuroImage 22, 1157–1172.
Pérez-González, D., Malmierca, M.S., Covey, E., 2005. Novelty detector neurons in the mammalian auditory midbrain. Eur. J. Neurosci. 22 (11), 2879–2885.
Pérez-González, D., Covey, E., Malmierca, M.S., 2008. Detection of novel sounds. Multiple manifestations of the same phenomenon? Rev. Neurol. 46 (2), 102–108.
Powers, R.K., Sawczuk, A., Musick, J.R., Binder, M.D., 1999. Multiple mechanisms of spike-frequency adaptation in motoneurones. J. Physiol. Paris 93, 101–114.
Rademacher, J., Morosan, P., Schormann, T., Schleicher, A., Werner, C., Freund, H.-J., Zilles, K., 2001. Probabilistic mapping and volume measurement of human primary auditory cortex. Neuroimage 13, 669–683.
Rao, R.P., Ballard, D.H., 1999. Predictive coding in the visual cortex: a functional interpretation of some extra-classical receptive-field effects. Nat. Neurosci. 2, 79–87.
Rinne, T., Alho, K., Ilmoniemi, R.J., Virtanen, J., Näätänen, R., 2000. Separate time behaviors of the temporal and frontal mismatch negativity sources. NeuroImage 12, 14–19.
Sams, M., Paavilainen, P., Alho, K., Näätänen, R., 1985. Auditory frequency discrimination and event-related potentials. Electroenceph. Clin. Neurophys. 62, 437–448.
Scherg, M., Von Cramon, D., 1985. Two bilateral sources of the late AEP as identified by a spatio-temporal dipole model. Electroencephalogr. Clin. Neurophysiol. 62 (1), 32–44.
Tiitinen, H., May, P., Reinikainen, K., Näätänen, R., 1994. Attentive novelty detection in humans is governed by pre-attentive sensory memory. Nature 372, 90–92.
Ulanovsky, N., Las, L., Nelken, I., 2003. Processing of low-probability sounds by cortical neurons. Nat. Neurosci. 6, 391–398.
Ulanovsky, N., Las, L., Farkas, D., Nelken, I., 2004. Multiple time scales of adaptation in auditory cortex neurons. J. Neurosci. 24 (46), 10440–10453.
Wager, T.D., Keller, M.C., Lacey, S.C., Jonides, J., 2005. Increased sensitivity in neuroimaging analysis using robust regression. NeuroImage 26, 99–113.
Winkler, I., Karmos, G., Näätänen, R., 1996. Adaptive modelling of the unattended acoustic environment reflected in the mismatch negativity event-related potential. Brain Res. 742, 239–252.